Towards a universal criteria for turbulence suppression in dilute turbidity currents with non-cohesive sediments

Mariano I. Cantero,[1] Mrugesh Shringarpure,[2] and S. Balachandar[2]

Received 29 May 2012; revised 22 June 2012; accepted 22 June 2012; published 27 July 2012.

[1] Turbidity currents exhibit fascinating physics as their sustained propagation depends on a tight interplay between the suspended sediments and turbulence. If resuspension dominates over deposition the intensity of the flow will increase, while if deposition dominates the flow turbulence can be completely damped inducing rapid settling of sediments and, eventually, flow extinction. This work explores the phenomenon whereby turbulence in a dilute turbidity current with non-cohesive sediments is abruptly extinguished owing to increased suspended sediment stratification. Three parameters control the flow dynamics: Reynolds number (Re_τ), Richardson number (Ri_τ) and sediment settling velocity ($\tilde{V}_z$). The condition for complete turbulence suppression can be expressed as a critical value for $Ri_\tau \tilde{V}_z$. Based on simulations, limited experiments and limited field data, the critical value appears to have a logarithmic dependence on Re_τ. **Citation:** Cantero, M. I., M. Shringarpure, and S. Balachandar (2012), Towards a universal criteria for turbulence suppression in dilute turbidity currents with non-cohesive sediments, *Geophys. Res. Lett.*, *39*, L14603, doi:10.1029/2012GL052514.

1. Introduction

[2] Turbidity currents derive their motion from the excess density imposed by suspended sediments. The increased density of the sediment-laden fluid creates a horizontal pressure gradient that drives the flow. If the flow is sufficiently intense turbulence is sustained. Flow turbulence is crucial since the enhanced shear stress at the bed enables resuspension. If resuspension dominates over deposition the current could self-accelerate [*Parker et al.*, 1986]. If deposition dominates, the intensity of the flow will decrease and will eventually extinguish [*Talling et al.*, 2007; *Cantero et al.*, 2012b].

[3] The governing equations of a dilute non-cohesive turbidity current flowing down a slope θ can be non-dimesionalized with H = current height as the length scale and shear velocity $u_* = \sqrt{\tau_b/\rho_f}$ as the velocity scale , where τ_b = bottom shear stress and ρ_f = fluid density. In the governing equations, three dimensionless parameters can be defined: Reynolds number (Re_τ), Richardson number (Ri_τ), and dimensionless sediment settling velocity ($\tilde{V}_z$)

$$Re_\tau = \frac{u_* H}{\nu}, \quad Ri_\tau = \frac{g_z R C^v H}{u_*^2} \quad \text{and} \quad \tilde{V}_z = \frac{V}{u_*}\cos\theta. \qquad (1)$$

Here $R = (\rho_p - \rho_f)/\rho_f$, ρ_p = sediments density, ν = kinematic viscosity which is taken as constant, V = settling velocity of an isolated sediment particle, C^v = mean volume concentration of suspended sediments, and $g_z = g\cos\theta$ = bed-normal component of gravity. A global balance of the driving force and the bottom shear stress yields $u_*^2 = RC^v H g_x$ (see also Figure S1 in auxiliary material), where $g_x = g\sin\theta$ = bed-tangential component of gravity.[1] Re_τ represents the ratio of inertial to viscous forces and thus measures the flow intensity. Stratification effects are proportional to the gradient of density. By expressing the above bulk Richardson number as $Ri_\tau = g_z R(C^v/H)/(u_*/H)^2$ it can be seen that it is a global equivalent of gradient Richardson number. Ri_τ represents the ratio between buoyancy and inertial forces and thus serves as a measure of stratification effects in momentum transfer. In a turbidity current the suspended sediments both drive and stratify the flow and thus the Richardson number becomes $Ri_\tau = 1/\tan\theta$ (see also Figure S1 in auxiliary material). The density gradients are measured by $\tilde{V}_z = \mathcal{Z}\kappa$ where $\mathcal{Z}$ is the Rouse number and κ is the von Karman constant. For the case of a field turbidity current of height H = 20 m running on a slope $\theta = 5°$ with a mean volume concentration C^v = 0.005 of 110 μm sand sediments in water (R = 1.65 and $\nu = 10^{-6}$ m^2/s), the above definitions give $Re_\tau = 7.5 \times 10^6$, $Ri_\tau = 11.43$ and $\tilde{V}_z = 2.3 \times 10^{-2}$.

[4] This work presents evidence to show that a turbidity current of fixed Re_τ remains turbulent provided the product $Ri_\tau \tilde{V}_z$ is below a threshold value. If either Ri_τ or $\tilde{V}_z$ is increased to go beyond the threshold, turbulence is completely extinguished and the flow eventually dissipates as sediments settle on the bed. A simple theoretical argument is presented to obtain $Ri_\tau \tilde{V}_z$ as the critical parameter. This product arises naturally as the dimensionless measure of turbulent kinetic energy (TKE) dissipation due to stable stratification. It is observed, however, that the damping of turbulence is weak until the threshold $Ri_\tau \tilde{V}_z$ is reached, beyond which turbulence is abruptly and completely damped. Turbulence damping can also be achieved in flows laden with cohesive sediments owing to their rheological effects [*Baas and Best*, 2002; *Sumner et al.*, 2009; *Baas*

[1] Bariloche Atomic Center, Institute Balseiro, CNEA, UNCu, National Council for Scientific and Technological Research, San Carlos de Bariloche, Argentina.

[2] Department of Mechanical and Aerospace Engineering, University of Florida, Gainesville, Florida, USA.

Corresponding author: M. I. Cantero, Bariloche Atomic Center, Institute Balseiro, CNEA, UNCu, National Council for Scientific and Technological Research, Bustillo 9500, San Carlos de Bariloche, Río Negro 8400, Argentina. (mcantero@cab.cnea.gov.ar)

0094-8276/12/2012GL052514

[1] Auxiliary materials are available in the HTML. doi:10.1029/2012GL052514.

Table 1. List of Direct Numerical Simulations (DNS)[a]

Case	Re_τ	Ri_τ	$\tilde{V}_z$	State
A-1	180	11.4	0.0	Turbulent
A-2	180	11.4	0.01	Turbulent
A-3	180	11.4	0.0255	Turbulent
A-4	180	11.4	0.0275	Turbulence suppressed
B-1	180	11.4	0.02125	Turbulent
B-2	180	11.4	0.023	Turbulence suppressed

[a]Set A: free-slip top boundary. Set B: no-slip top boundary.

et al., 2009]. The present work addresses only turbidity currents driven by non-cohesive sediments, and one of the novelties is to show that complete turbulence suppression can also be achieved in dilute turbidity currents ($C^v \lessapprox 1\%$) owing to stratification effects. Past research has mostly focused on density stratification by scalars like temperature or salinity [see *Armenio and Sarkar*, 2002]. In contrast the settling tendency of the sediments skews the stratification effects towards the bed inducing a break of symmetry in the flow [*Cantero et al.*, 2009b, 2009a].

[5] Numerical results and laboratory observations [*Sequeiros et al.*, 2009] indicate the threshold $Ri_\tau \tilde{V}_z$ to be between 0.25 to 0.5 for low to moderate Re_τ. In comparison, field occurrences of turbidity currents are at Re_τ orders of magnitude larger [*Xu et al.*, 2004; *Hay et al.*, 1982]. Recent results on Re_τ scaling of TKE production and dissipation [*Laadhari*, 2002] are employed in this work to propose a similar scaling for buoyancy-induced turbulence damping, which yields a logarithmic dependence for threshold $Ri_\tau \tilde{V}_z$ on Re_τ.

2. Methods

[6] Following *Cantero et al.* [2009a], a simplified model for the body of a turbidity current is considered as an inclined channel in which the flow is driven by granular non-cohesive sediments of uniform size, finite settling velocity and negligible inertia. The flow is assumed dilute ($C^v \lesssim 1\%$) so that interaction between sediment particles and rheology effects can be neglected, Boussinesq approximation can be employed (density of the current is slightly higher than the ambient fluid and therefore it is acknowledged only via the body force term in the governing equation), and settling velocity is independent of concentration. The settling velocity can be computed employing, for example, Dietrich's formula [see *Garcia*, 2008, p. 41]. Employing scales H, u_* and C^v the dimensionless set of equations that describes the flow are [*Cantero et al.*, 2009a]

$$\frac{\partial \tilde{\mathbf{u}}}{\partial \tilde{t}} + \tilde{\mathbf{u}} \cdot \nabla \tilde{\mathbf{u}} = -\nabla \tilde{p} + \frac{1}{Re_\tau} \nabla^2 \tilde{\mathbf{u}} + \tilde{c}\mathbf{e}_x - Ri_\tau \tilde{c}\mathbf{e}_z, \nabla \cdot \tilde{\mathbf{u}} = 0, \quad (2)$$

$$\frac{\partial \tilde{c}}{\partial \tilde{t}} + \left(\tilde{\mathbf{u}} + \tilde{V}_x\mathbf{e}_x - \tilde{V}_z\mathbf{e}_z\right) \cdot \nabla \tilde{c} = \frac{1}{Re_\tau Sc} \nabla^2 \tilde{c}, \quad (3)$$

where $\tilde{\mathbf{u}}$ = dimensionless fluid velocity, $\tilde{c}$ = dimensionless volume concentration of sediments, $\tilde{p}$ = dimensionless pressure, $Sc = \nu/\mathcal{D}$ = Schmidt number with $\mathcal{D}$ the diffusivity of sediments employed to model resuspension from the bed, $\tilde{V}_x = V \sin\theta/u_*$, and $\mathbf{e}_x$ and $\mathbf{e}_z$ = unit vectors in the streamwise and bed-normal directions. These equations are solved using a de-aliased pseudospectral code on a grid $N_x = 96 \times N_y = 96 \times N_z = 97$ in the streamwise, spanwise and bed-normal directions. Periodic boundary condition are employed in the streamwise and spanwise directions. For velocity, no-slip has been imposed at the bottom boundary, while free-slip (set A in Table 1) and no-slip (set B in Table 1) have been employed for the top boundary (see also Figure S2 in auxiliary material). The initial conditions for the simulations are turbulent channel flow velocity field and a well-mixed concentration field.

[7] The dynamics of sediment resuspension is very complex [*García and Parker*, 1993; *Sánchez and Redondo*, 1997; *Medina et al.*, 2001] and still not well understood. In the DNS, sediment resuspension is incorporated by means of the diffusion term on the right hand side of (3). This diffusion in non-cohesive sediments arise from their long range hydrodynamic interaction [*Segre et al.*, 2001]. The boundary condition imposed for concentration is zero total flux at the top and bottom boundaries, thus conserving the total amount of suspended sediments and allowing the flow to reach steady state. When turbulence is damped, the sediments are sequestered in a thin, near-bed zone, whose thickness can be expected to grow due to deposition since the basal shear stress is not sufficient to resuspend sediments. However, when turbulence is maintained, the thickness of this layer remains fixed. The development of high-concentration basal layers is not accounted by this model. More details on the mathematical model and its implementation can be found in *Cantero et al.* [2007b, 2007a, 2009a].

[8] It is worth mentioning that DNS provides complete three-dimensional time-dependent information of the velocity, pressure and concentration fields, and no turbulence modeling is required. Mean variables are computed as averages over planes parallel to the bed and over time. Derived variables such as TKE and dissipation are directly computed from their definitions, with no assumptions.

3. Evidence of Turbulence Suppression

[9] This section presents evidence for the abrupt change in flow behavior. Results from two sets of simulations listed in Table 1 are presented. The range of $\tilde{V}_z$ and Ri_τ employed in the simulations are of the order of values presented in section 1 for a typical field turbidity currents, with the exception of $Re_\tau = 180$. Although Re_τ in the simulations is much smaller than in field cases, the resulting turbidity currents are fully turbulent when stratification effects are weak. In this regards, one of the main objectives of this work is to shed light on the Reynolds scaling of stratification effects on turbidity currents to allow extrapolation of present DNS results.

[10] Figure 1a shows the bed-normal variation of the mean concentration profiles. The results for set A show an abrupt change in behavior as $\tilde{V}_z$ increases from 0.0255 to 0.0275. For $\tilde{V}_z \leq 0.0255$ the flow remains turbulent and the sediments concentration remains nearly uniform, except close to the top and bottom boundaries where the sediment diffusion dominates over turbulent mixing to balance the settling flux. For $\tilde{V}_z = 0.0275$ the concentration profile shows an exponential decay consistent with the laminar solution of (3). The behaviors for $\tilde{V}_z = 0.02125$ and 0.023 of set B are quite different and consistent with the abrupt suppression of

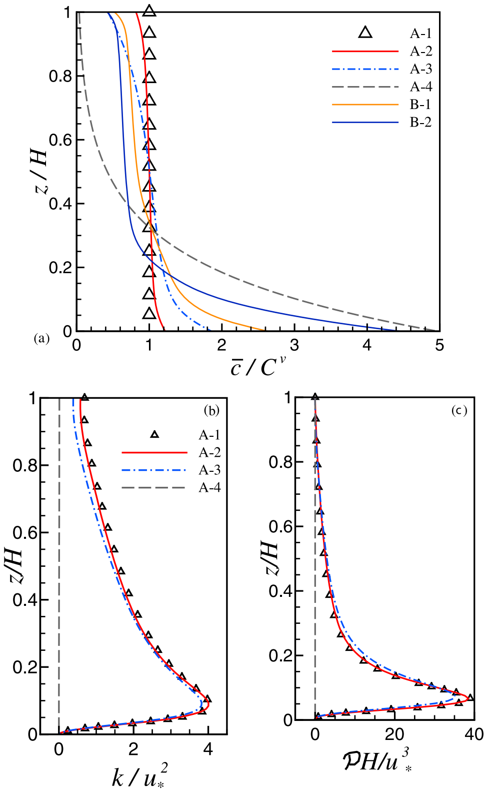

Figure 1. Bed-normal profiles of (a) mean volume concentration; (b) dimensionless turbulent kinetic energy (k/u_*^2); (c) dimensionless turbulent kinetic energy production ($\mathcal{P}H/u_*^3$). Results for cases listed in Table 1. See definition in (6). The turbulent kinetic energy measures the turbulence intensity of the flow, and the turbulent kinetic energy production measures the ability of the flow to continue creating turbulence.

turbulence at some $\tilde{V}_z$ in between. With increasing $\tilde{V}_z$, the sediment concentration near the bottom boundary increases contributing to stronger stable stratification effects.

[11] The abrupt nature of turbulence suppression can be better appreciated in Figures 1b and 1c where the TKE and TKE production (see precise definition in (6) of section 4) profiles are plotted for all cases of set A. When compared to pure channel flow (case A-1), the influence of increasing sediment settling on TKE is quite small for $\tilde{V}_z \leq 0.0255$. An abrupt change can be clearly seen as $\tilde{V}_z$ increases to 0.0275. For case A-4 both TKE and TKE production are completely damped across the entire fluid layer. The results of set B also show such an abrupt change, however, not as clear owing to continued TKE production at the top boundary. The critical $\tilde{V}_z$ for complete turbulence suppression is comparable for the two configurations, illustrating relative insensitivity to details away from the bottom boundary. Figure 1 is for Ri_τ = 11.4 and similar threshold behavior is observed for other Ri_τ. Also for a fixed non-dimensional sediment settling velocity there exists a critical Ri_τ beyond which the flow turbulence is completely suppressed.

[12] Direct observation of complete turbulence suppression and complete settling of sediments is hard to achieve in laboratory flumes. Recent experiments [*Sequeiros et al.*, 2009], however, have documented self-accelerating flows to transition and become depositional with increasing sediments size, providing support to the threshold behavior.

4. Theoretical Considerations

[13] The parametric grouping controlling the observed sharp transition to complete turbulence suppression can be derived from the following analysis. Consider a steady dilute turbidity current with only non-cohesive sediments in equilibrium where resuspension and deposition at the bed are in balance, and ambient fluid entrainment at the top interface is negligible [*Cantero et al.*, 2009a]. Then, the governing equations of the mean flow are:

$$\frac{d}{dz}\left(-\overline{u'w'} + \nu\frac{d\overline{u}}{dz}\right) + \overline{c}Rg_x = 0, \quad \frac{d}{dz}\left(\overline{c'w'} - \overline{c}V_z\right) = \mathcal{D}\frac{d^2\overline{c}}{dz^2} \quad (4)$$

$$\mathcal{P} - \epsilon + \frac{d}{dz}\left[\nu\frac{dk}{dz} - \overline{w'\left(\frac{p'}{\rho_c} + \frac{1}{2}u'_iu'_i\right)}\right] + \overline{c'u'}Rg_x - \overline{c'w'}Rg_z = 0. \quad (5)$$

Here u (=u_1) and w (=u_3) = streamwise and bed-normal flow velocity, p = pressure, c = sediments volume concentration, bars and prime represent mean and perturbations, and

$$k = \frac{1}{2}\overline{u'_iu'_i}, \quad \mathcal{P} = -\overline{u'w'}\frac{d\overline{u}}{dz}, \quad \epsilon = \nu\overline{\frac{\partial u'_i}{\partial x_i}\frac{\partial u'_i}{\partial x_i}} \quad (6)$$

are the TKE, TKE production and TKE dissipation. In the last term of (4) left, the suspended sediments drive the mean flow and the forcing is dictated by the concentration profile $\overline{c}(z)$. In (5) the last two terms embody the damping influence of suspended sediments.

[14] Equations (4) can be integrated to

$$u_*^2 = RC^vHg_x \quad \text{and} \quad \overline{c'w'} = \overline{c}V_z + \kappa\frac{d\overline{c}}{dz}, \quad (7)$$

where $C^v = 1/H\int_0^H \overline{c}dz$.

[15] Employing (7), (5) can be integrated to its dimensionless form

$$\tilde{P} - \tilde{\varepsilon} + \frac{1}{Re_\tau}\left(\frac{d\tilde{k}}{d\tilde{z}}\Big|_0^1 + \frac{Ri_\tau}{Sc}\zeta\right) = Ri_\tau\tilde{V}_z + \beta, \quad (8)$$

where

$$\tilde{P} = \frac{1}{u_*^3}\int_0^H \mathcal{P}dz, \quad \tilde{\varepsilon} = \frac{1}{u_*^3}\int_0^H \epsilon dz, \quad \beta = -\frac{1}{HC^vu_*}\int_0^H \overline{c'u'}dz,$$
$$\text{and} \quad \zeta = \frac{\overline{c}_b - \overline{c}_t}{C^v} \quad (9)$$

are the dimensionless bed-normal-integrated TKE production and dissipation, β is a component of TKE damping, and $\overline{c}_t$ and $\overline{c}_b$ are the top and bottom boundary concentrations. Here, tilde means dimensionless variables.

[16] Equation (8) dictates the global TKE balance and the two terms on the right account for the TKE consumption to maintain sediments in suspension. When the

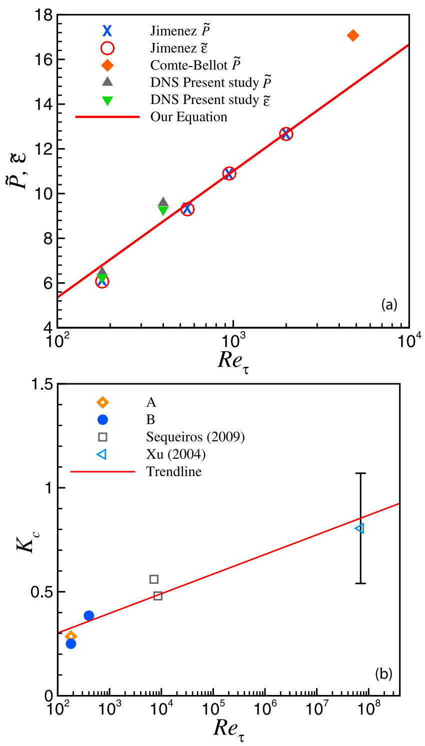

Figure 2. (a) Evolution of bed-normal-integrated turbulent kinetic energy production and dissipation with Re_τ. Data labeled as Jimenez taken from *Hoyas and Jimenez* [2006], and data labeled Comte-Bellot taken from *Laadhari* [2002]. (b) Evolution of K_c with Re_τ. Data points are obtained from our DNS cases, experiments and field observations. The data for this plot is shown in Table 2. A trend line is fitted through scattered data points to show the logarithmic dependence of K_c on Re_τ.

availability of TKE to maintain the sediments in suspension is not enough, net sedimentation occurs and the flow extinguishes eventually. In this work $Ri_\tau \tilde{V}_z$ is proposed to capture total TKE consumption to maintain sediments in suspension, since β is observed to be ≈30% of $Ri_\tau \tilde{V}_z$ in all the cases considered. Therefore, the condition for complete turbulence suppression is $Ri_\tau \tilde{V}_z > K_c$, where K_c is the critical value beyond which suspended sediments completely extinguish turbulence.

5. Reynolds Number Scaling

[17] For the two sets of simulations in Table 1, K_c is computed to range from 0.25 to 0.313. Corresponding results for the higher $Re_\tau = 400$ yield K_c in the range 0.35 to 0.39 [*Cantero et al.*, 2012a], thus exhibiting a weak Re_τ dependence. It is of interest to scale these results to very large Re_τ of relevance to field scale turbidity currents.

[18] As displayed in Figures 1b and 1c, as long as the flow remains turbulent, turbulence statistics shows only a weak dependence on $\tilde{V}_z$. This is consistent with the fact that for case A-3 $\tilde{P} = 6.6$ and $Ri_\tau \tilde{V}_z + \beta = 0.397$, i.e., sediment-induced TKE comsumption is only ≈6% of $\tilde{P}$. The Re_τ scaling for K_c is thus sought from the Re_τ dependence of TKE in a pure turbulent channel flow without sediments. In this limit $\tilde{\mathcal{P}}$ can be exactly expressed as [*Zanoun and Durst*, 2009]

$$\tilde{\mathcal{P}} = Re_\tau (g(\tilde{z}) - \tilde{z})(1 - g(\tilde{z})) \quad \text{where} \quad g(\tilde{z}) = -\overline{\tilde{u}'\tilde{w}'} + \tilde{z}. \tag{10}$$

Recent investigations [*Laadhari*, 2002, 2007] have shown peak TKE production to scale linearly as Re_τ, but the location of the peak to scale as Re_τ^{-1}. To obtain an estimate of $\tilde{P}$ the empirical function [*Panton*, 2007]

$$g(\tilde{z}) = \frac{2}{\pi}\arctan\left(\frac{0.82 Re_\tau \tilde{z}}{\pi}\right)\left[1 - \exp\left(-\frac{Re_\tau \tilde{z}}{7.8}\right)\right]^2 \tag{11}$$

is used. Integrating (10) $\tilde{P} \approx 2.46 \ln(Re_\tau) - 5.97$.

[19] Figure 2a shows the above scaling along with the simulation results for turbulent channel flow [*Hoyas and Jimenez*, 2006], and results from two of our turbidity current simulations: (i) $Re_\tau = 180$, $Ri_\tau = 11.4$, $\tilde{V}_z = 0.015$ and (ii) $Re_\tau = 400$, $Ri_\tau = 2.5$, $\tilde{V}_z = 0.175$. While TKE dissipation balances production in the absence of sediments (as $Re_\tau \to \infty$), their difference is small in a turbidity current and is balanced by $Ri_\tau \tilde{V}_z + \beta$.

[20] Based on the results above, a logarithmic scaling of K_c is postulated. Laboratory and field data for turbidity currents reported in Table 2 is used to validate this hypothesis. The laboratory experiments by *Sequeiros et al.* [2009] were performed in a 15 m-long flume with a 5% slope, and correspond to a continuous current loaded with non-cohesive plastic particles ranging from 20 to 200 μm. The evolution of particle concentration and the speed of the current at downstream locations were monitored to categorize the current into self accelerating, depositional and autosuspension. The values for *Xu et al.* [2004] correspond to observations of turbidity currents in the Monterrey Canyon, west of California, USA. Velocity measurements were performed with acoustic Doppler current profilers (ADCP), and sediment concentrations have been estimated to be lower than 0.05. The sediments can be considered fine sand.

[21] It must be recognized, however, that the above field observations and laboratory experiments were not conducted

Table 2. Experimental and Field Observations Used in Figure 2b[a]

Case	H	C^v	S	d	R	V_z	Re_τ	K_c
Sequeiros et al. [2009][b]	0.33	7.8×10^{-2}	5.0×10^{-2}	20–200	0.3	1.2	7.2×10^3	0.56
Sequeiros et al. [2009][c]	0.36	8.5×10^{-2}	5.0×10^{-2}	20–200	0.3	1.1	8.6×10^3	0.48
Xu et al. [2004]	60–100	$<5.0 \times 10^{-2}$	$>10^{-2}$	100	1.65	7.5	7.0×10^7	0.54–1.07

[a]Current half-height has been used as length scale. Current height H expressed in m, sediments diameter d expressed in μm, and settling velocity V_z expressed in mm/s.
[b]Test 11, data for x = 4.8 m and settling velocity refers to the concentration-weighted values.
[c]Test 11, data for x = 14.3 m and settling velocity refers to the concentration-weighted values.

with the goal of establishing the threshold value of K_c. As a result, some of the information needed in the calculation of K_c was not measured or reported, in which case we estimate a plausible range of values and compute the corresponding range of K_c in Table 2. Also, the limiting equilibrium state between self-accelerating and depositional flow (called auto-suspension mode) is taken here to be the critical stage before turbulence suppression. Experimental and field observations thus interpreted are shown in Figure 2b where values of K_c are plotted against Re_τ. This figure also includes the simulation results for Re_τ = 180 and 400. The best fit is $Ri_\tau \tilde{V}_z|_{crit} = K_c(Re_\tau) \approx 0.041 \ln(Re_\tau) + 0.11$.

[22] The experimental and field data show a definite upward trend, but exhibit considerable scatter. Thus, the scaling for K_c is intended as a guideline. Clearly, additional higher Re_τ simulations and experiments with a focus on observing turbulence suppression by stratification are needed.

[23] At low Reynolds numbers additional Re_τ dependence may arise. As can be seen from (8), the diffusive term is negligible for large Re_τ, but may represent a significant sink of TKE at lower Re_τ. Thus, low Re_τ simulations are inadequate to obtain asymptotic scaling. For pure channel flow $Re_\tau \gtrsim 500$ was required for the viscous effect to be negligible in the production-dissipation balance [*Laadhari*, 2007].

6. Conclusions

[24] In dilute turbidity currents, non-cohesive suspended sediments have two effects: a) to drive the flow and supply energy for turbulence, and b) to create stable density stratification and suppress turbulence. These two competing effects are characterized by three parameters: Re_τ, Ri_τ and $\tilde{V}_z$. A critical value of $Ri_\tau \tilde{V}_z$ is observed to exist, beyond which turbulence is completely extinguished by stratification. From the TKE equation the parametric grouping $Ri_\tau \tilde{V}_z$ is theoretically obtained, which can be interpreted as the energy spent to keep sediments in suspension. Simulations show that the transition is abrupt and happens when only about 6% of the bed-normal-integrated TKE production is consumed to maintain sediments in suspension. For values of $Ri_\tau \tilde{V}_z$ lower than criticality the effect of suspended sediments on turbulence remains small, but once exceeded turbulence is completely turned off. In a channel flow the bed-normal-integrated TKE production and dissipation scale as $\ln(Re_\tau)$, based on which a logarithmic dependence for critical $Ri_\tau \tilde{V}_z$ with increasing Re_τ is proposed. Laboratory and field observations, along with present results are used to obtain a best fit for this Re_τ dependence. It has been shown that turbulence damping can be achieved by rheology effect in turbidity current carrying sufficient amount of cohesive sediments [*Baas and Best*, 2002]. This work shows that complete turbulence suppression can also be achieved due to stratification effects in dilute (volume average concentration $C^v \lesssim 1\%$) non-cohesive turbidity currents.

References

Armenio, V., and S. Sarkar (2002), An investigation of stably stratified turbulent channel flow using large-eddy simulation, *J. Fluid Mech.*, *459*, 1–42.

Baas, J. H., and J. L. Best (2002), Turbulence modulation in clay-rich sediment-laden flows and some implications for sediment deposition, *J. Sediment. Res.*, *72*, 336–340.

Baas, J. H., J. L. Best, J. Peakall, and M. Wang (2009), A phase diagram for turbulent translational and laminar clay suspension flows, *J. Sediment. Res.*, *79*, 162–183.

Cantero, M. I., S. Balachandar, and M. H. Garcia (2007a), High-resolution simulations of cylindrical density currents, *J. Fluid Mech.*, *590*, 437–469, doi:10.1017/S0022112007008166.

Cantero, M. I., J. R. Lee, S. Balachandar, and M. Garcia (2007b), On the front velocity of gravity currents, *J. Fluid Mech.*, *586*, 1–39, doi:10.1017/S0022112007005769.

Cantero, M. I., S. Balachandar, A. Cantelli, C. Pirmez, and G. Parker (2009a), Turbidity current with a roof: Direct numerical simulation of self-stratified turbulent channel flow driven by suspended sediment, *J. Geophys. Res.*, *114*, C03008, doi:10.1029/2008JC004978.

Cantero, M. I., S. Balachandar, and G. Parker (2009b), Direct numerical simulation of stratification effects in a sediment-laden turbulent channel flow, *J. Turbul.*, *10*(27), 1–28, doi:10.1080/14685240903159197.

Cantero, M. I., S. Balachandar, A. Cantelli, and G. Parker (2012a), Extinction of near-bed turbulence due to self-stratification in turbidity currents: The dependence on shear Reynolds number, in *Environmental Fluid Mechanics*, *IAHR Monogr.*, edited by W. Rodi and M. Uhlmann, p. 456, CRC press, Boca Raton, Fla.

Cantero, M. I., A. Cantelli, C. Pirmez, S. Balachandar, D. Mohrig, T. A. Hickson, T. Yeh, H. Naruse, and G. Parker (2012b), Emplacement of massive turbidites linked to extinction of turbulence in turbidity currents, *Nat. Geosci.*, *5*(1), 42–45.

García, M., and G. Parker (1993), Experiments on the entrainment of sediment into suspension by a dense bottom current, *J. Geophys. Res.*, *98* (C3), 4793–4807, doi:10.1029/92JC02404.

Garcia, M. H. (Ed.) (2008), *Sedimentation Engineering: Processes, Measurements, Modeling, and Practice*, *ASCE Manuals Rep. Eng. Pract.*, vol. 110, Am. Soc. of Civ. Eng., Reston, Va.

Hay, A. E., R. W. Burling, and J. W. Murray (1982), Remote acoustic detection of a turbidity-current surge, *Science*, *217*(4562), 833–835.

Hoyas, S., and J. Jimenez (2006), Scaling of the velocity fluctuations in turbulent channels up to Re_τ = 2003, *Phys. Fluids*, *18*(1), 011702, doi:10.1063/1.2162185.

Laadhari, F. (2002), On the evolution of maximum turbulent kinetic energy production in a channel flow, *Phys. Fluids*, *14*(10), L65–L68, doi:10.1063/1.1511731.

Laadhari, F. (2007), Reynolds number effect on the dissipation function in wall-bounded flows, *Phys. Fluids*, *19*(3), 038101, doi:10.1063/1.2711480.

Medina, P., M. Sánchez, and J. Redondo (2001), Grid stirred turbulence: Applications to the initiation of sediment motion and lift-off studies, *Phys. Chem. Earth, Part B*, *26*(4), 299–304, doi:10.1016/S1464-1909(01)00010-7.

Panton, R. L. (2007), Composite asymptotic expansions and scaling wall turbulence, *Philos. Trans. R. Soc. A*, *365*(1852), 733–754, doi:10.1098/rsta.2006.1951.

Parker, G., Y. Fukushima, and H. M. Pantin (1986), Self-accelerating turbidity currents, *J. Fluid Mech.*, *171*, 145–181.

Sánchez, M., and J. Redondo (1997), Observations from grid stirred turbulence. Grid characterization and application to sediment lift-off experiments, *Appl. Sci. Res.*, *59*, 243–254, doi:10.1023/A:1001139623537.

Segre, P. N., F. Liu, P. Umbanhowar, and D. A. Weitz (2001), An effective gravitational temperature for sedimentation, *Nature*, *409*, 594–597.

Sequeiros, O. E., H. Naruse, N. Endo, M. H. Garcia, and G. Parker (2009), Experimental study on self-accelerating turbidity currents, *J. Geophys. Res.*, *114*, C05025, doi:10.1029/2008JC005149.

Sumner, E. J., P. J. Talling, and L. A. Amy (2009), Deposits of flows transitional between turbidity current and debris flow, *Geology*, *37*(11), 991–994, doi:10.1130/G30059A.1.

Talling, P. J., et al. (2007), Onset of submarine debris flow deposition far from original giant landslide, *Nature*, *450*(7169), 541–544, doi:10.1038/nature06313.

Xu, J. P., M. A. Noble, and L. K. Rosenfeld (2004), In-situ measurements of velocity structure within turbidity currents, *Geophys. Res. Lett.*, *31*, L09311, doi:10.1029/2004GL019718.

Zanoun, E., and F. Durst (2009), Turbulent momentum transport and kinetic energy production in plane-channel flows, *Int. J. Heat Mass Transfer*, *52*(17–18), 4117–4124, doi:10.1016/j.ijheatmasstransfer.2009.03.046.